Analysis of Deep-Stall Characteristics of *T*-Tailed Aircraft Configurations and Some Recovery Procedures

RAYMOND C. MONTGOMERY* AND MARTIN T. MOUL†
NASA Langley Research Center, Hampton, Va.

Some *T*-tail aircraft designs may be susceptible to pitch-up and a subsequent trim at an extreme angle of attack from which recovery is difficult. Such a condition is called a deep stall and is a result of an aft center-of-gravity position, nonlinear pitching-moment characteristics, and the low level of elevator control effectiveness available at high angles of attack with some airplane designs. An investigation of deep-stall characteristics and recovery techniques was made using phase-plane techniques to solve the equations of motion for nonlinear aerodynamic characteristics typical of these configurations. Results of the phase-plane analyses were expressed in the form of static and dynamic recovery margins that yield a quantitative measure of recovery capability. Static recovery is defined as recovery from deep stall by application of full stick forward elevator deflection. Dynamic recovery is defined as recovery obtained by pulsing the elevator back and forth so as to build up pitching velocity. A comparison of analytical and simulator results showed a good correlation of dynamic recovery margin and simulator recoveries.

Nomenclature

A_n = peak amplitudes of pitch damping functions
$\bar{c}$ = wing mean aerodynamic chord, ft
C_L = lift coefficient, $L/\bar{q}S$
C_m = pitching-moment coefficient, $M/\bar{q}S\bar{c}$
$C_{m_{\delta_e}}$ = $\partial C_m/\partial\delta_e$
C_{m_q} = $\partial C_m/\partial(q\bar{c}/2V)$
q = pitch rate, rad/sec
$\bar{q}$ = dynamic pressure, psf
D = drag, lb
h = altitude, ft
I_y = pitch moment of inertia, slug-ft^2
k_y = radius of gyration in pitch, ft
K_y = $k_y/\bar{c}$
L = lift
m = mass, slugs
M = pitching moment, ft-lb
M_q = $\partial M/\partial q$
S = wing area
T = thrust, lb
V = freestream velocity, fps
W = weight, lb
SRM = static recovery margin
DRM = dynamic recovery margin
α = angle of attack, deg or rad
γ = flight-path angle, deg
δ_e = elevator deflection, deg or rad
ϵ = inclination of thrust axis to body axis, deg
θ = angle of pitch, deg or rad
μ = relative density parameter, $m/\rho S\bar{c}$
ρ = atmospheric density, slugs/ft^3

Subscripts

cr = critical
ds = deep stall
dy = maximum, stick back elevator
ue = unstable equilibrium

A dot over a variable denotes time differentiation.

Presented as Preprint 66-13 at the AIAA 3rd Aerospace Sciences Meeting, New York, January 24–26, 1966; submitted February 7, 1966; revision received June 20, 1966.

* Aero-Space Technologist, Astromechanics Branch, Space Mechanics Division.

† Aerospace Engineer, Astromechanics Branch, Space Mechanics Division. Member AIAA.

Introduction

PITCH-UP and deep-stall characteristics of *T*-tail aircraft with engines mounted on the rear of the fuselage have been the subject of recent investigations at Langley Research Center. Aerodynamic characteristics of a general class of *T*-tail airplanes and dynamic and recovery characteristics in the deep stall have been reported in Refs. 1 and 2, respectively. Whereas the deep-stall characteristics presented in Ref. 2 were the results of a fixed-base simulator study, this paper describes an analytical method and recovery criteria for defining deep-stall characteristics. Because the pitching-moment characteristics of *T*-tail aircraft are extremely nonlinear with angle of attack (for example, Ref. 1), phase-plane techniques are used for the analysis, in which airplane pitching motions are presented as plots of pitching velocity against angle of attack. Two types of recovery procedures are considered. Static recovery is defined as recovery with application of full stick forward elevator deflection. As wind-tunnel tests have indicated a large reduction in pitch damping in the deep stall for such airplane configurations, the possibility of dynamic recovery is suggested. With this technique, the elevator is pulsed back and forth so as to build up pitching oscillations and produce recovery. For the assumed control procedures, recovery capability was assessed for aerodynamic characteristics similar to those of *T*-tail configurations to determine effects of variations in the pitching-moment curve and pitch damping. Results for some specific characteristics are compared with simulator results[2] to show the applicability of the technique. The technique described could be a useful design tool for preliminary analysis of deep-stall characteristics. However, final conclusions as to recovery capability of specific airplane configurations should always be based on more complete analyses, such as pilot simulator studies.

The physical problem to be analyzed herein can be introduced with the aid of Fig. 1, a plot of airplane pitching-moment coefficient vs angle of attack. A combination of a near-stall flight condition, an aft center-of-gravity location, and an inadvertent large elevator deflection can cause a severe pitch-up and a resulting pitch trim at a high angle of attack (the deep stall). If, with stick forward elevator deflection, a region of positive pitching moment exists in the deep stall, then a locked-in-trim condition may exist, and recovery may

be impossible. The analysis of attempted recovery from such conditions is the subject of this paper.

Analysis

System Equations

The primary motion of concern in the deep stall is the severe pitch-up to an extreme angle of attack and the recovery from a possible high angle-of-attack trim condition. Possible recovery techniques that come to mind utilize elevator, aileron, or rudder inputs. For example, examination has shown that rudder and aileron inputs might be applied to intentionally sideslip or roll the airplane to take advantage of a nose-down pitching moment due to sideslip, or a decrease in angle of attack as a result of rolling motions. However, such yawing and rolling maneuvers are considered in the category of last resort attempts because of the poor lateral and directional stability and control characteristics anticipated at these extreme angles of attack. With this assumption, the following three-degree-of-freedom analysis of longitudinal motions was undertaken, neglecting the lateral modes of motion. A requirement of the analysis is that the airplane pitching-moment curves, damping in pitch, and control effectiveness be treated as nonlinear functions of angle of attack.

The appropriate equations of motion (stability axis system) are

$$m\dot{V} = T\cos(\alpha + \epsilon) - D - W\sin\gamma \quad (1)$$

$$mV\dot{\gamma} = L + T\sin(\alpha + \epsilon) - W\cos\gamma \quad (2)$$

$$I_y\dot{q} = M_q q + M(\alpha, \delta_e) \quad (3)$$

In the simulator study of Ref. 2, it was observed that an airplane trimmed at a deep-stall angle of attack maintained a constant, steep glide path. In addition, the stall entries were performed with idle thrust. For these assumed conditions $\gamma = T = 0$, Eq. (2) reduces to

$$L = C_L\bar{q}S = W\cos\gamma_0 \quad (2a)$$

In addition,

$$q = \dot{\alpha} \quad (4)$$

and

$$\theta = \alpha + \gamma_0 \quad (5)$$

with

$$\dot{q} = q(dq/d\alpha) \quad (6)$$

Equation (3) is reduced to

$$\frac{dq}{d\alpha} = \frac{M(\alpha, \delta_e) + M_q(\alpha)q}{I_y q} \quad (3a)$$

Furthermore, the variation of atmospheric density with altitude is neglected, so that

$$\rho = \rho_0 \quad (7)$$

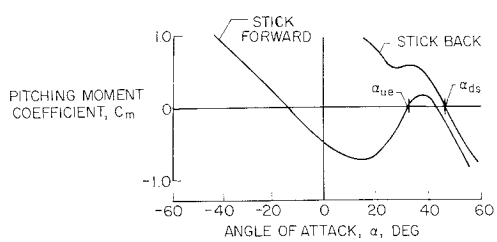

Fig. 1 Typical pitching-moment curves for a T-tail aircraft.

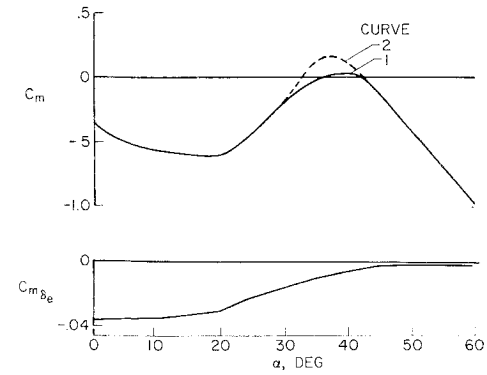

a) Pitching-moment curve and elevator effectiveness

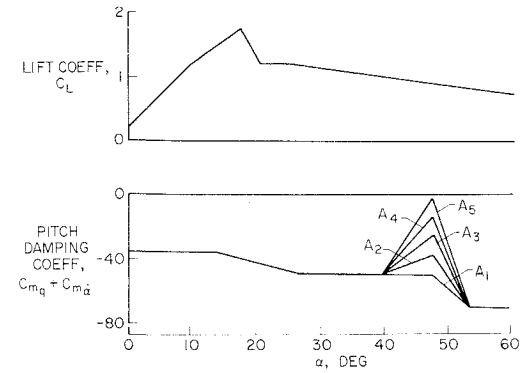

b) Lift curve and pitch damping

Fig. 2 Airplane aerodynamic characteristics.

from which

$$V = (2\bar{q}/\rho_0)^{1/2} \quad (8)$$

To summarize, the system equations employed in this analysis are Eqs. (2a, 3a, 4, and 8).

Before proceeding to the solutions of the equations, it is necessary to consider the assumed airplane aerodynamic characteristics for deep-stall conditions.

Aerodynamic Characteristics

The aerodynamic characteristics assumed herein were taken from wind-tunnel results of a general study of T-tail airplane configurations reported in Ref. 1 and as such are not representative of any existing aircraft. These pitching-moment characteristics, elevator effectiveness, lift characteristics, and damping in pitch are presented as functions of angle of attack in Fig. 2. Pitching-moment curves are for stick forward elevator deflection with an aft center-of-gravity position at 40% $\bar{c}$, and they define two arrangements included in the analysis, both of which possess a high angle-of-attack trim point. Of course, curve 2 with its larger positive moment coefficients will present a more difficult recovery situation because of the larger nose-up potential energy it possesses, as represented by the area under the curve for which $C_m > 0$. The variation of elevator effectiveness with angles of attack is a significant factor in this problem because of the very low control power available in the deep stall. The lift curve exhibits a typical variation with angle of attack, with lift increasing gradually until wing stall occurs. After experiencing an appreciable loss of lift at stall, the lift gradually decreases with further increase in angle of attack. Tests of T-tail configurations conducted in the Langley 8-ft Transonic Pressure Tunnel showed that a large reduction in pitch damping ($C_{m_q} + C_{m_{\dot{\alpha}}}$) might be expected in the deep stall, and consequently variations in pitch damping were included for assessment. Five damping functions were as-

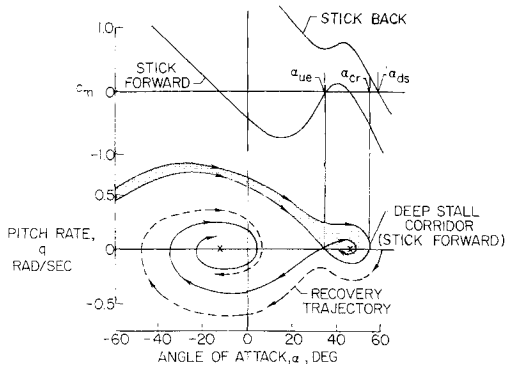

Fig. 3 Phase plane trajectories for stick-forward elevator deflection.

sumed and are shown in Fig. 2. For comparison, constant damping values ($C_{m_q} + C_{m_{\dot{\alpha}}}$) of -35 to -70 were also considered.

Phase-Plane Trajectories

The system equations are solved for aerodynamic characteristics (Fig. 2) considered typical of T-tail aircraft that possess a deep-stall trim capability. Solutions are obtained as phase-plane trajectories, and an illustrative one is presented in Fig. 3. A phase-plane trajectory is a plot of the state of a system for a given control function and in this problem consists of pitching velocity and angle-of-attack conditions for a given elevator deflection. The system motion in response to any initial condition is determined by spotting the initial dynamic conditions on the phase-plane figure and then constructing a trajectory parallel to a system of reference trajectories that have been precomputed for the given control condition. Solutions for a family of control functions, in this problem elevator deflections, permit an analysis of the control and stability of the system. In Fig. 3, two pitching-moment curves for stick forward and stick back elevator deflections are presented together with the phase-plane plot of q vs α for *only* stick forward elevator deflection. Inspection of the stick forward moment curve reveals three equilibrium or trim points, two being stable (for which $dC_m/d\alpha$ is negative) and the third unstable. These equilibrium points appear in the phase plane as two nodes and one saddle point. All phase-plane trajectories (for this particular elevator deflection) must eventually converge to one of the two nodes, and particular trajectories are shown (solid lines) which pass through the unstable equilibrium point α_{ue}. This angle is a crossover point between nose-up and nose-down pitching motions, and trajectories originating at this point form boundaries that divide the phase plane into regions for which specific trajectories will converge to one or the other node. [However, the actual shapes of the trajectories at $\alpha < 20°$ are of questionable validity because of the constraint of constant flight-path angle assumed for the analysis. As the normal range of angle of attack is restored ($\alpha < 20°$), flight-path angle will decrease, and the assumption of constant flight-path angle will be violated. This is of little importance to this problem, as the region of specific interest here is at high angle of attack.] The shaded region is the one for which motions will damp to the high angle-of-attack, or deep-stall, trim point. For disturbances or elevator control inputs that produce excursions into the deep stall, the shaded region indicates conditions for which recovery to operational angles of attack (5°–10°) could not be achieved with full nose-down (stick forward) control. The remainder of the paper will consider the problem of recovery from the deep stall with two types of piloting techniques being considered.

Recovery Margins

Two possible piloting techniques involving elevator control for recovery from deep stall are considered herein. The first technique to be described is termed "static recovery."

In Fig. 3 are presented pitching-moment curves of an assumed configuration for stick forward and stick back elevator deflections and phase-plane trajectories associated with the stick forward elevator deflection. Two angles of specific interest to recovery are shown α_{ds} and α_{cr}. The trim angle of attack for stick back elevator deflection is α_{ds}, whereas α_{cr} is the minimum trim angle of attack from which recovery can be accomplished with stick forward elevator deflection. For the pitching-moment characteristics depicted in Fig. 3, $\alpha_{ds} > \alpha_{cr}$, and, from an initial condition of trimmed flight at α_{ds} (for stick back elevator deflection), recovery will be accomplished by an abrupt change of control to stick forward elevator deflection with the recovery motion approximating the dashed curve. Although transient motions are produced in such a recovery, this piloting technique is said to cause static recovery. This terminology is used to distinguish this recovery technique from the second one to be considered. To summarize, then, static recovery requires $\alpha_{ds} > \alpha_{cr}$. Obviously, the acceptability of recovery motions depends on the margin by which α_{ds} exceeds α_{cr}, and a nondimensional static recovery margin (SRM) has been arbitrarily defined which is useful for comparing effects of parametric changes. Static recovery margin is defined as

$$\text{SRM} = (\alpha_{ds} - \alpha_{cr})/(\alpha_{cr} - \alpha_{ue})$$

where the denominator is an arbitrary nondimensionalizing factor. Examination of the formula shows that SRM $= 0 = \alpha_{ds} - \alpha_{cr}$ defines the recovery boundary and that positive values ($\alpha_{ds} > \alpha_{cr}$) are required for recovery.

The curves of Fig. 3 illustrate the importance of elevator effectiveness to deep-stall recovery. The elevator effectiveness assumed in Fig. 3 is not typical of T-tail configurations. Reference to Fig. 2 shows that elevator effectiveness $C_{m\delta_e}$ reduces to a very small value in the deep stall, and it is to be expected that $\alpha_{ds} < \alpha_{cr}$ for most configurations of interest.

In conditions for which static recovery is not possible, recovery may possibly be effected by a technique of rapidly cycling the elevator control back and forth between nose-down and nose-up elevator so as to build up pitching oscillations and finally pitch down to normal angles of attack. Such a technique is termed "dynamic recovery."

The capability for dynamic recovery is determined from a phase-plane plot in which trajectories for both stick back and stick forward elevator deflections are superimposed. Figure 4 is an example of such recovery, in which pertinent trajectories of Fig. 3 for stick forward elevator are presented, as well as trajectory for stick back elevator (dashed curve). The particular trajectory of interest for stick back elevator is one that passes through α_{ue} and spirals into deep-stall trim, α_{ds}. Then, a square wave program of elevator deflection in which the switching is performed at $q = 0$ with nose-down control applied during negative (nose down) pitching and nose-up

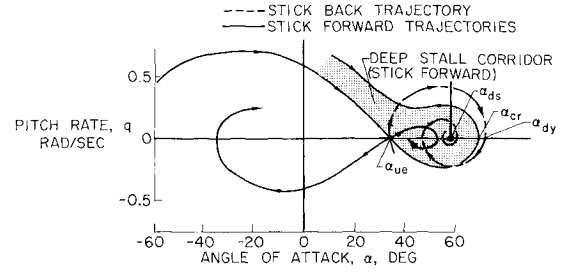

Fig. 4 Phase plane trajectories for both stick-forward and stick-back elevator deflections.

control applied during positive (nose up) pitching will produce recovery if $\alpha_{dy} > \alpha_{cr}$. Again, a nondimensional recovery margin can be defined with which the recovery capabilities of classes of configurations can be compared. Thus, dynamic recovery margin (DRM) is defined as

$$\text{DRM} = (\alpha_{dy} - \alpha_{cr})/(\alpha_{cr} - \alpha_{ue})$$

where the denominator is reference value. Examination of the formula shows that DRM = 0 = $\alpha_{dy} - \alpha_{cr}$ defines the recovery boundary and that positive values ($\alpha_{dy} > \alpha_{cr}$) indicate recovery.

Results and Discussion

Results are presented to show the effects of airplane pitching-moment curve, pitch damping, and airplane relative density on deep-stall recovery. Nonlinear pitching-moment curves and angle-of-attack variations of elevator effectiveness and pitch damping as presented in Fig. 2 were all considered in the analysis. Variations in relative density have been introduced to illustrate some general effects of airplane size. Results are presented in terms of the relative density parameter μ, defined by $\mu = m/\rho Sc$. Assumptions included in consideration of relative density effects were W/S = const and K_y = const. For reference, the largest airplane considered had a gross weight of 130,000 lb, a mean aerodynamic chord of 15.7 ft, and a wing area of 1700 ft², for which μ = 100 at an altitude of 15,000 ft. The results to be presented for relative density variations are applicable for airplane size variation only, with μ varying inversely with airplane length by virtue of the preceding assumptions.

Results are presented in Fig. 5 to show the effect of damping variations on recovery for pitching-moment curve 1 (defined in Fig. 2). The damping values used are the five nonlinear functions of Fig. 2. The figure shows that static recovery is not possible, dynamic recovery is possible for all but the A_1 damping function, and a reduction in damping in the deep stall is beneficial to dynamic recovery. It is considered that such damping variations would be more effective in improving static recovery capability if the region of reduced damping occurred at a somewhat lower angle of attack, between α_{ue} and α_{ds}. The significant point here is that the technique of dynamic recovery may yield a recovery from the deep stall for conditions in which static recovery is not possible.

Effects of pitching-moment curve on recovery are presented in Fig. 6 for the same relative density (167) as Fig. 5. The pitching-moment curves used are those designated 1 and 2 in Fig. 2. From an inspection of the moment curves, recovery for curve 2 would be expected to be more difficult because of the larger nose-up moments to be overcome, and such is the case. The effect of moment curve 2 is to produce a more negative static recovery margin and also a negative dynamic recovery margin.

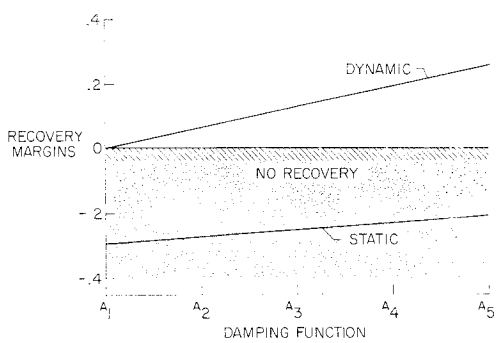

Fig. 5 Effect of pitch damping on recovery margins; pitching-moment curve 1 (μ = 167).

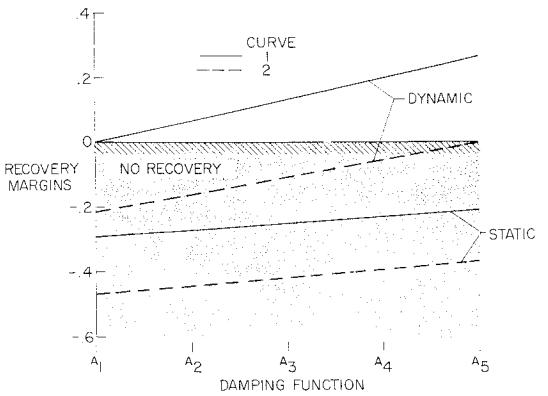

Fig. 6 Effect of pitching-moment curve on recovery margins (μ = 167).

Although the pitch-up characteristics of T-tail commercial jet transports have recently received attention, smaller business and executive class aircraft of this type have received little attention. For this reason, it appeared desirable to include in this analysis some results for airplane size variations, and results are presented in Fig. 7 for values of relative density parameter (μ) of 100 to 500 for a constant damping in pitch (C_{m_q}) of −40. The pitching-moment characteristics included are those of curve 1. With increase in μ, both recovery margins increase positively; however, the static recovery margin remains negative for all airplane sizes. The dynamic recovery margin is about zero for μ of 100 and increases with size reduction to a large value (0.45) for μ of 500.

Results have been presented herein based on two piloting techniques that have been idealized as the result of two assumptions. One assumption is that elevator deflections can be introduced instantaneously, whereas in practice elevator servos have a finite deflection rate capability. The second assumption is that elevator inputs are made precisely at zero value of pitching velocity for the dynamic recovery technique. In practice, such idealized pilot performance cannot be expected. In spite of these limitations, there is felt to be merit in such analyses, and comparisons have been made with the fixed-base simulator results of Ref. 2 for the same configurations. In Fig. 8 are presented results of comparable configurations as percent of recoveries in the simulator, against static and dynamic recovery margins. Admittedly the data are meager, but some trends are evident.

First, no correlation of simulator recoveries is seen with the static recovery margin, for with a static recovery margin of −0.2 all of the simulator runs recovered. However, good correlation is indicated with the dynamic recovery margin with the simulator recovery boundary falling in the vicinity

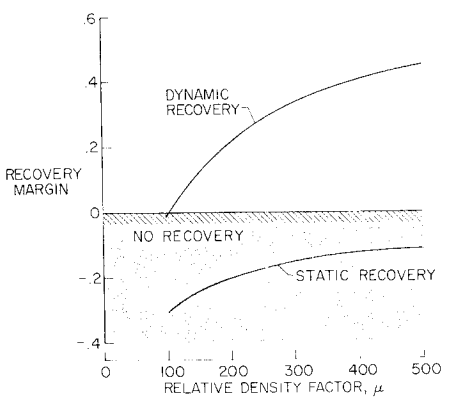

Fig. 7 Effect of airplane relative density factor on recovery margins for constant C_{m_q} of −40.

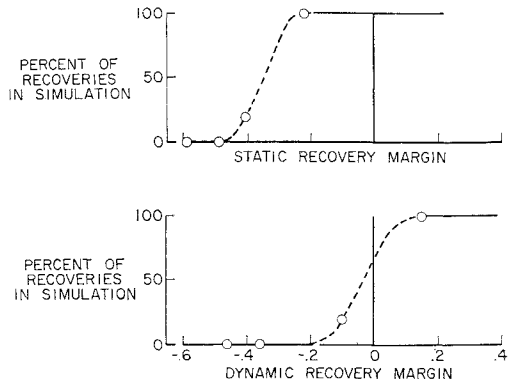

Fig. 8 Comparison of recovery results of simulator and analytical studies.

of zero dynamic recovery margin, as might be expected. Actually, the pilot technique used in the simulator is more nearly one of dynamic recovery in that the pilots first applied nose-down elevator while still pitching up to attempt recovery. If unsuccessful, they would then resort to pulsing the elevator up and down, as assumed in this analysis. The correlation is considered good, particularly since the simulator results were obtained prior to the analytical study and the pilot tasks were not selected so as to demonstrate static or dynamic recovery. For example, an apparent inconsistency appears in Fig. 8 in that a small percent of recoveries were accomplished with a negative recovery margin of -0.1. These few recoveries were obtained because pilots initiated corrective action at a prescribed rate of descent, and in these runs deep-stall angles of attack were not attained. The simulator results indicate that the concept of dynamic recovery is meaningful and demonstrate that recovery can be effected for positive values of dynamic recovery margin.

Conclusions

A method has been developed for analyzing deep-stall recovery characteristics of T-tail airplane configurations possessing nonlinear pitching-moment and damping curves.

From phase-plane trajectories for fixed elevator deflections, two recovery criteria were developed for assessing deep-stall recovery. One criterion, for static recovery, assumes that full stick forward elevator deflection is applied. The second criterion, for dynamic recovery, assumes a pilot attempt at pumping the airplane out of the deep stall by alternate forward and aft deflections of the stick. The application of the method to a range of airplane characteristics produced the following conclusions:

1) Dynamic recovery is shown to be a significant recovery technique for the deep stall, in that it provides recovery capability for many conditions in which static recovery is not possible.

2) Good correlation is obtained between dynamic recovery margin and simulator results of deep-stall recovery, indicating the validity of the dynamic recovery technique as a possible emergency procedure for recovery from deep stall.

3) Consideration of the difficulties that can be encountered in application of the dynamic recovery technique and of the possible large losses of altitude accompanying such recovery dictate, from safety considerations, that aircraft be designed to possess static recovery capability.

References

[1] Taylor, R. T. and Ray, E. J., "A systematic study of the factors contributing to post-stall longitudinal stability of T-tail configurations," AIAA Paper 65-737 (1965).

[2] Lina, L. J. and Moul, M. T., "A simulator study of T-tail aircraft in deep stall conditions," AIAA Paper 65-781 (1965).